JGR Atmospheres

RESEARCH ARTICLE
10.1029/2023JD039928

Key Points:

- Locally measured Biogenic volatile organic compound (BVOC) emission factors were used to update BVOC emissions in south China
- Updated lower regional BVOC emissions improved model prediction of O_3 when compared to surface monitoring
- Modeled O_3 and secondary organic aerosol concentrations became lower with the updated BVOC emissions in south China

Supporting Information:

Supporting Information may be found in the online version of this article.

Correspondence to:

Y. Zhang,
zhang_yl86@gig.ac.cn

Citation:

Wang, P., Zhang, Y., Gong, H., Zhang, H., Guenther, A., Zeng, J., et al. (2023). Updating biogenic volatile organic compound (BVOC) emissions with locally measured emission factors in south China and the effect on modeled ozone and secondary organic aerosol production. *Journal of Geophysical Research: Atmospheres*, *128*, e2023JD039928. https://doi.org/10.1029/2023JD039928

Received 8 SEP 2023
Accepted 4 DEC 2023
Corrected 4 JAN 2024

This article was corrected on 4 JAN 2024. See the end of the full text for details.

Author Contributions:

Conceptualization: Yanli Zhang, Alex Guenther, Tao Wang, Xinming Wang
Data curation: Haixing Gong, Hongliang Zhang, Jianqiang Zeng
Formal analysis: Peng Wang, Yanli Zhang, Jianqiang Zeng, Tao Wang
Funding acquisition: Yanli Zhang
Investigation: Peng Wang, Yanli Zhang, Tao Wang
Methodology: Peng Wang, Yanli Zhang, Haixing Gong, Hongliang Zhang, Alex Guenther, Jianqiang Zeng, Tao Wang, Xinming Wang

Updating Biogenic Volatile Organic Compound (BVOC) Emissions With Locally Measured Emission Factors in South China and the Effect on Modeled Ozone and Secondary Organic Aerosol Production

Peng Wang[1], Yanli Zhang[2], Haixing Gong[1], Hongliang Zhang[3,4,5], Alex Guenther[6], Jianqiang Zeng[2], Tao Wang[7], and Xinming Wang[2]

[1]Department of Atmospheric and Oceanic Sciences, Fudan University, Shanghai, China, [2]State Key Laboratory of Organic Geochemistry and Guangdong Key Laboratory of Environmental Protection and Resources Utilization, Guangzhou Institute of Geochemistry, Chinese Academy of Sciences, Guangzhou, China, [3]Institute of Eco-Chongming (IEC), Shanghai, China, [4]IRDR ICoE on Risk Interconnectivity and Governance on Weather/Climate Extremes Impact and Public Health, Fudan University, Shanghai, China, [5]Shanghai Key Laboratory of Atmospheric Particle Pollution and Prevention, Department of Environmental Science and Engineering, Fudan University, Shanghai, China, [6]Department of Earth System Science, University of California, Irvine, Irvine, CA, USA, [7]Department of Civil and Environmental Engineering, Hong Kong Polytechnic University, Hong Kong, China

Abstract Biogenic volatile organic compounds (BVOCs) emitted from terrestrial plants contribute substantially to ozone (O_3) and secondary organic aerosol (SOA) formation in the troposphere. Accurate estimation of BVOC emissions is highly challengeable with a variety of uncertainties, one of which is the use of default emission factors (EFs) particularly for underrepresented regions without local data. In this study, locally measured BVOC-EFs in south China, a subtropical region with abundant vegetation, were used to update regional BVOC emissions as estimated by the Model of Emissions of Gases and Aerosols from Nature (MEGAN). These EFs were recently determined in situ with characterized dynamic chambers for the emissions of isoprene, monoterpenes, and sesquiterpenes from tree species. The Community Multiscale Air Quality (CMAQ) model was then employed to see how much the regional O_3 and SOA production is altered with the updated BVOC emissions. Results revealed lower BVOC emission estimates in south China when using the localized EFs than the MEGAN default ones, particularly for sesquiterpenes with a notable average reduction rate of approximately 40%. Using the updated BVOC emissions improved model O_3 predictions in all seasons when compared to surface O_3 monitoring, yet the lower BVOC emissions resulted in modeled O_3 and SOA concentrations decreased by up to −6 ppb and −1.5 μg m^{-3}, respectively, throughout south China. This study highlights the significance of localized EFs in refining emission estimates and air quality predictions in regions with a wealth of vegetation.

Plain Language Summary Terrestrial plants can emit a variety of biogenic volatile organic compounds (BVOCs), such as isoprene and terpenes. These BVOCs significantly impact tropospheric ozone (O_3) and secondary organic aerosol (SOA) formation, and therefore accurate BVOC emission estimates are crucial for air quality modeling particularly in regions with a wealth of vegetation. However, in many regions local BVOC emission factors (EFs) are unavailable and using the model default EFs may bias the regional BVOC emissions. Here we carried out in situ measurements of EFs with well characterized dynamic chambers in south China. With these local EFs, the BVOC emissions was estimated by the MEGAN model, revealing a reduction in BVOC emissions in south China than those using the default EFs. When compared the modeling results with those from surface monitoring network, model performance in the prediction of O_3 was improved with updated BVOC emissions incorporated into the air quality modeling. Additionally, our modeling outcomes illustrated that by using the updated BVOC emissions, predicted O_3 and SOA levels could be notably reduced in specific regions. This study highlights the importance of integrating region-specific data to enhance the precision of BVOC emission estimates and improve air quality predictions, particularly in regions with abundant vegetation.

Project Administration: Yanli Zhang
Resources: Yanli Zhang, Xinming Wang
Software: Peng Wang, Haixing Gong, Hongliang Zhang
Supervision: Yanli Zhang, Xinming Wang
Validation: Peng Wang, Hongliang Zhang
Writing – original draft: Peng Wang
Writing – review & editing: Peng Wang, Yanli Zhang, Alex Guenther, Tao Wang, Xinming Wang

1. Introduction

The biogenic volatile organic compounds (BVOCs) are regarded as the most important precursor to secondary organic aerosols (SOA) and ozone (O_3) due to their high reactivity with the key oxidants such as hydroxyl (OH) radical and large amounts of emissions (Fuentes et al., 2000; Tuazon & Atkinson, 1990). Globally, the BVOCs play the dominant role compared to the anthropogenic sources, contributing 75%–90% of the total VOC emissions (Fuentes et al., 2000; Guenther et al., 1995). Especially in China, the average BVOC emissions reached up to 34 Tg per year from 2001 to 2016, further enhancing the formation of secondary pollutants (Wang et al., 2021a; Zhang et al., 2007). In the summertime, the contribution of BVOCs to SOA was up to 74% in China, far exceeding the contribution from anthropogenic emissions (Wang et al., 2018). Therefore, it is significant to study the variabilities of BVOC emissions in China to determine their impacts on air quality.

The emission flux models such as the Model of Emissions of Gases and Aerosols from Nature (MEGAN) and Biogenic Emission Inventory System (BEIS) are widely used to estimate the BVOC emissions (Guenther et al., 1995, 2012; Vukovich & Pierce, 2002). In these models, the BVOC emissions are determined by complex factors, including ambient temperature, radiation, CO_2 concentrations, land-use and emission factors (EFs), which may lead to differences of approximately dozens of times among different studies in BVOC estimations (Carlton & Baker, 2011; Emmerson et al., 2020; Guenther et al., 2012; Hantson et al., 2017; Jiang et al., 2018; Li et al., 2020a, 2020b). Particularly, previous study stated the changes in land-use led to a 11.4% increase in BVOCs in China, and thus induced −10 to +20% and −20 to +30% changes in O_3 and SOA concentrations, respectively (Fu & Liao, 2014). Most of these factors are well-studied (Bash et al., 2016; Fu & Liao, 2014; Guenther et al., 1993; Huang et al., 2015; Lun et al., 2020; Oderbolz et al., 2013; Opacka et al., 2021; Pressley et al., 2006; Sharkey et al., 1999; Wang et al., 2021b). For instance, Zhang et al. (2018) found that using satellite photosynthetically active radiation could improve the accuracy of BVOC estimation by increasing the correlation coefficient from 0.93 to 0.97. Ma et al. (2019) reported that higher temperature increased the BVOC emissions and then aggravated the O_3 concentration (up to 4.74 ppb) in the North China Plain (NCP) in China.

However, scant attention has been devoted to standard emission factors (EFs) of BVOCs in China (Lun et al., 2020). In general, EFs are derived from different plant functional types (PFTs) and their uncertainties are considered the major contributor to the total BVOC emissions estimate uncertainty (Guenther et al., 2012; Misztal et al., 2016). Remarkably, EFs exhibit significant variability even within the same plant species. For instance, isoprene EFs from oak trees range from 39 to 258 μgC g^{-1} h^{-1}, a range 2 to 28 times greater than previous estimations for the same species (Geron et al., 2001). In addition, the EFs also show prominent regional characteristics due to the different land-use and vegetation composition (Wang et al., 2011). Bai et al. (2015) underscored this fact, reporting measured EFs for isoprene and monoterpenes 12% and 20% lower than MEGAN default values in a temperate mixed forest in Northern China, respectively Moreover, improving the BVOC EFs also helped enhance the model performance. Wang et al. (2017) updated the MEGAN EF modules and significantly improved the isoprene prediction by reducing the mean fractional bias (MFB) from 0.91 to −0.11. As a result, an in-depth EFs study is required to better evaluate the BVOC emissions in China.

In recent decades, China leads in world greening, resulting from a series of land-use management plans (Chen et al., 2019), and contributes approximately 25% of the net increase in leaf area from 2000 to 2017. This burgeoning greenery potentially amplifies BVOC emissions, which in turn could exert notable effects on air quality, particularly in regions like south China, characterized by elevated BVOC emissions (Cao et al., 2022; Fu & Liao, 2014). A recent study pointed out that the BVOC emissions in south China increased by approximately 8.6%–11.7% in south China in 2013–2016 compared to 2001–2004 (Wang et al., 2021a). These higher BVOC emissions further led to a rapid increment of O_3 in the Pearl River Delta (PRD) in south China (Cao et al., 2022). However, studies considering locally-measured EFs in south China have remained largely stagnant for over a decade (Leung et al., 2010; Tsui et al., 2009; Wang et al., 2011), which hardly represents recent changes in BVOC emissions. Thus, it is urgent to carry out a comprehensive study of BVOCs emissions with the updated EFs to re-evaluate the BVOC emissions and their impact on air quality in south China.

In this study, we updated the EFs of major BVOC species, including isoprene, monoterpene, and sesquiterpene in the MEGAN model in south China, which is based on recent in situ measurements in the PRD region (Zeng et al., 2022a). A source-oriented CMAQ model was applied to quantify their contributions to O_3 and SOA formation. The temporal and spatial variations of BVOCs were discussed in this study. We aim to re-evaluate the BVOC emissions and their impacts on ozone and secondary organic aerosol formation in south China.

Table 1
The New-Localized Standard BVOC EFs (μg m^{-2} hr^{-1}) for MEGAN

BVOCs	Species	Broadleaf	Needleleaf	Brush
Isoprene	Isoprene	10,206.3 (10,000)	263.5 (600)	1,932.5 (2,000)
Monoterpenes	Myrcene	37.3 (30)	56.2 (70)	47.8 (30)
	Sabinene	32.3 (50)	195.7 (70)	79.7 (50)
	Limonene	85.2 (80)	261.1 (100)	127.6 (60)
	3-Carene	16.4 (30)	271.8 (160)	47.8 (30)
	t-β-Ocimene	61.6 (120)	28.7 (70)	143.5 (90)
	β-Pinene	68.7 (130)	335.4 (300)	159.5 (100)
	α-Pinene	249.7 (400)	523.0 (500)	318.9 (100)
	Other Monoterpenes	64.2 (150)	73.9 (180)	175.4 (110)
Sesquiterpenes	Farnesene	24.3 (40)	12.3 (40)	63.8 (40)
	β-Caryophyllene	25.5 (40)	14.6 (80)	79.7 (50)
	Other Sesquiterpenes	50.2 (40)	79.2 (120)	159.5 (100)

Note. The number in parenthesis is the global average MEGAN EFs (as default model input).

2. Methods

2.1. BVOC EFs Development for MEGAN Model

Based on recent in situ measurements in Guangdong province (GD), a new BVOC EF database was developed for the MEGAN model. The field measurements were conducted from September 2019 to March 2021. A total of 15 broadleaf tree species and 5 needleleaf tree species were measured at the branch level, which covered the dominated tree types in GD. According to the 9th National Forest Census in China (http://www.forestdata.cn/, last access in May 2022), the major tree species were *Pinus massoniana Lamb.*, *Pinus elliottii Engelm.,* and *Cunninghamia lanceolate (Lamb.) Hook*. for needleleaf trees, and *Quercus., Cinnamomum camphora (L.) Presl.,* and *Eucalyptus robusta Smith.* for broadleaf trees. The detailed information of the in situ measurements could be found in Zeng et al. (2022a).

Equation 1 was applied to convert the measured EFs from the branch to the canopy level under the standard conditions to meet the requirements of the MEGAN model (Purser et al., 2021; Wang et al., 2016):

$$EF = E \times SLA_i \times LAI_i \quad (1)$$

where EF (μg m^{-2} h^{-1}) and E (μg g^{-1} h^{-1}) are the BVOC EFs from the MEGAN model and in situ measurement, respectively. SLA (g m^{-2}) and LAI (m^2 m^{-2}) stand for the specific leaf weight and the leaf area index for vegetation type *i*, respectively. Typically, the SLA values are 100, 150, 175 g m^{-2}, and the LAI values are 5, 5, 2 m^2 m^{-2} for the broadleaf, needleleaf, and shrubs, respectively (Wang et al., 2011; Zheng et al., 2010). By combining the recently measured BVOC EFs in Zeng et al. (2022a) with measurements from previous studies in this region, a new-localized BVOC EF database was obtained (Bai et al., 2001; Baker et al., 2005; Huang et al., 2011; Leung et al., 2010; Tsui et al., 2009). This new-localized EFs database contained three major BVOCs including isoprene, monoterpene, and sesquiterpene. Moreover, the explicit VOC species of monoterpene and sesquiterpene categories were also considered in this study as shown in Table 1.

2.2. Model Setup and Application

In this study, a source-oriented CMAQ model was used to quantify the impacts of the updated BVOC EFs and the contribution of BVOC emissions on air quality in south China (Wang et al., 2019). The SAPRC-11 (S11L) photochemical mechanism with updated isoprene reactions was coupled in the CMAQ model (Carter & Heo, 2013; Ying et al., 2015). The simulation periods were January, April, July, and October 2019 to investigate BVOC seasonal variations and matched the time of the associated field study (as mentioned in Section 2.1). To get better model performance, a nested domain setup was applied with horizontal resolutions of 36 km (China

and part of East Asia) and 12 km (south China, Figure S1 in Supporting Information S1), and the domain details were described in Wang et al. (2021c). In this study, we utilized the default ICON/BCON programs to generate initial and boundary conditions for the 36 km simulation, which represented a clean continental condition. For the 12 km simulation, the initial condition was obtained from the default ICON program, while the boundary condition was derived from the results of the 36 km simulation. Meteorological parameters were simulated by the Weather Research and Forecasting (WRF) model version 4.2.1, driven by the National Centers for Environmental Prediction (NCEP) Final (FNL) reanalysis data (National Centers for Environmental Prediction/National Weather Service/NOAA/U.S. Department of Commerce, 2015) (ds083.3, https://rda.ucar.edu/datasets/ds083.3/, last accessed: May 2022). Anthropogenic emissions were from the Multi-resolution Emission Inventory for China (Zheng et al., 2021) (MEIC, http://meicmodel.org/, last accessed: May 2022) year 2019, and Emissions Database for Global Atmospheric Research (EDGAR, https://edgar.jrc.ec.europa.eu/, last accessed: May 2022) year 2015 for China and other countries, respectively. The biogenic emissions were generated by the MEGAN model version 2.1 (Guenther et al., 2012). To determine the changes by using the updated BVOC EFs, two sets of BVOC emissions were considered: (a) using the global average EFs from the MEGAN model (BASE case), and (b) using the new local-localized EFs mentioned in Section 2.1 (NEF case). Due to the vegetation diversity, EFs were substituted in the entire Guangdong province where the local EFs were measured in the NEF case (Zeng et al., 2022a).

3. Results and Discussions

3.1. WRF-CMAQ Model Evaluation

Meteorological perimeters play a key role in the estimation of BVOC emissions and the formation and transportation of pollutants (Guenther et al., 2012). The major hourly meteorological parameters, including temperature at 2 m (T2), wind speed and wind direction at 10 m (WS and WD), and relative humidity (RH) predicted by the WRF model, were used to conduct the model validation. The observation data were from the National Climatic Data Center (https://www.ncei.noaa.gov/products/land-based-station/integrated-surface-database, last accessed: May 2023), which had a total of 185 sites in south China. In general, the WRF model has a well performance based on the statistical indicators shown in Table S1 in Supporting Information S1, which is also comparable with previous studies (Hu et al., 2016; Liu & Wang, 2020; Wang et al., 2021a). For example, the T2 predictions in all months have met the criteria (Emery et al., 2001) except for the mean bias (MB) in April. The T2 has the best model performance (MB = 0.0) in July when the BVOC emissions are high. The predicted T2 can provide firm inputs for the MEGAN model since it is considered as the main environmental factor that divers the BVOC emissions (Guenther et al., 2012). The WRF model over-predicts the WS in all months, as indicated by the positive MB values ranging from 0.3 to 0.7. This higher WS may enhance the regional transport of air pollutants. RH is slightly under-predicted in January and April but overestimated in July and October, suggesting by the variations in the MB values. In January, the predicted RH is 75.0% compared to 79.1% in the observation, and in April this underestimation gets alleviated.

In addition, the CMAQ model also provides a well prediction of the key pollutants compared to the observation from the National Air Quality Monitoring Network (Zhu, 2022) (https://figshare.com/articles/dataset/Observational _data/21709265/1, last accessed: March 2022, a total of 253 sites in the nested 12km domain). For both BASE and NEF cases, the predicted O_3 and $PM_{2.5}$ have all captured the seasonal variations of the observation and satisfied the criteria (Tables S2 and S3 in Supporting Information S1) (EPA, 2005, 2007). In particular, the highest O_3 concentration occurs in October but in January for $PM_{2.5}$ in south China. Similar to the meteorological evaluation, the best CMAQ model performance is found in July, suggesting the model is able to give robust results during the high BVOC emission season. For both simulation cases, the CMAQ model slightly overestimates the O_3 concentration. On average, O_3 predictions from NEF cases are closer to observations. From January to October, the O_3 mean normal bias (MNB) values are 0.09, 0.09, 0.01, 0.0 for the NEF case, and 0.12, 0.17, 0.05, and 0.02 for the BASE case. We further separate the observation sites into three categories as PRD (within the PRD region, 56 sites), noPRD (outside PRD but within Guangdong province, 50 sites), and noGD (outside Guangdong province, 148 sites) according to their locations to comprehensively evaluate the model performance (Figure S2 in Supporting Information S1). In all these sites, the predictions in NEF case alleviate the overestimation in O_3 that is commonly reported in the air quality model when compared with the BASE case (Yang & Zhao, 2023) (Figure S3 in Supporting Information S1). The lower O_3 in PRD and noPRD sites from the NEF is due to the

changes in the BVOC emission, which further help to reduce the overestimation of O_3 in the noGD sites through regional transport. Particularly, in spring, the predicted O_3 from the NEF case is 3 ppb lower on average than that of the BASE case in Guangdong province (including both PRD and noPRD sites), leading to a 5 ppb reduction in the noGD sites. In contrast, the CMAQ model predicts lower $PM_{2.5}$ concentrations in both cases in all site categories (Figure S4 in Supporting Information S1). The average predicted $PM_{2.5}$ concentrations are 30.4 and 29.4 μg m^{-3} for BASE and NEF cases, respectively, compared to 34 μg m^{-3} of the observation. In January and April, the under-predicted $PM_{2.5}$ may be partially attributed to the lower RH from the WRF model. Previous also reported that RH posed a significant impact on $PM_{2.5}$ concentrations in winter and spring (Chen et al., 2020). Besides the BVOC emissions and metrological parameters, other factors such as the anthropogenic emissions and the simulation resolution also affect the $PM_{2.5}$ prediction. A previous study reported that using different anthropogenic emissions also leads to a distinct difference in $PM_{2.5}$ and its component (Wang et al., 2018). Thus, a time-efficient anthropogenic emission with a high resolution is required to further improve the model prediction.

3.2. Comparison of BVOCs in NEF and BASE Cases

3.2.1. Comparison of BVOC EFs

As shown in Table 1, the NEF cases show obvious differences with the global average MEGAN EFs. The dominant PFTs in the study domain are needleleaf evergreen temperate trees (up to ∼80%) and broadleaf deciduous temperate trees (up to ∼60%, Figure S5 in Supporting Information S1), so their EFs are selected to represent needleleaf and broadleaf categories, respectively. The impacts of the shrubs and bushes type are negligible since this vegetation type distributes sporadically with little coverage (<5%) in the study domain.

The new-localized isoprene EFs (10,206 μg m^{-2} h^{-1}) are slightly higher than the MEGAN global average value (10,000 μg m^{-2} h^{-1}) of the broadleaf function type, while they are 1.96 times the value (5,200 μg m^{-2} h^{-1}) reported in the previous study in the PRD region (Wang et al., 2011). Opposite results are found in the needleleaf type. The new-localized needleleaf EFs are 1.3 and 2.0 times lower than that of the global MEGAN model and a previous study in the PRD (Wang et al., 2011), respectively. On a regional scale, the NEF case has the lower isoprene in the PRD and its surrounding regions with a difference of over −3,000 μg m^{-2} h^{-1} compared to the BASE case (Figure 1). This may help to improve the model performance of isoprene, as a recent study reported that the MEGAN model overestimated isoprene emissions by 20%–30% in the PRD region (Zhang et al., 2020). The higher isoprene EFs (>4,000 μg m^{-2} h^{-1}) of the NEF case are predicted in scattered locations with more broadleaf coverage, such as Shaoguan and Qingyuan in GD.

The changes in monoterpene EFs varied by individual species (Table 1). Generally, the NEF case predicts a lower monoterpene EFs than the BASE case and Wang et al. (2011) for the broadleaf type, except for the myrcene and limonene. For instance, the β-pinene EF is 68.7 μg m^{-2} h^{-1} in the NEF case, which is only 53% and 21% of the BASE and the value in Wang et al. (2011), respectively. For the needleleaf type, the NEF case has larger EFs for most monoterpene species rather than the BASE case. Specifically, the limonene EF is 261.1 μg m^{-2} h^{-1}, which is 2.6 times of the BASE case. In addition, different monoterpene species of the NEF case also show different spatial distributions (Figure 1). For α-pinene, the high EFs are located in the north of GD, which is 50% larger than the BASE case. While the β-pinene EFs are ubiquitously lower than the BASE case throughout GD. The NEF derived the lower sesquiterpene EFs in both broadleaf and needleleaf types than the BASE case. Especially in the needleleaf type, the β-caryophyllene EFs in the NEF case are only 18% (14.6 μg m^{-2} h^{-1}) of the BASE case, and thus leads to a lower EFs in the entire GD (Figure 1). This lower sesquiterpene EF is partially attributed to the underestimation during the field measurements, which was reported in previous studies (Zeng et al., 2022a, 2022b). In addition, the SLA used in Equation 1 can also induce significant differences in all BVOC EFs estimations (Guenther et al., 2020). In this study, the SLA is determined by the tree genera, such as the broadleaf type, but there are many diverse species even within one tree genera. This may also bring uncertainties in the calculation of SLA since it varies with tree species and environmental factors (Liu et al., 2017).

3.2.2. Comparison of BVOC Emissions and Concentrations

In general, the NEF case estimates lower BVOC emissions than the BASE case in the study domain (Figure 2). The most significant difference is found in sesquiterpene emissions, with an average reduction rate of over −40% in the NEF case. In contrast, the average reduction rates of isoprene and monoterpene emissions are less than 5%. In both BASE and NEF cases, isoprene emerges as the dominant BVOCs throughout the year. During summer, its

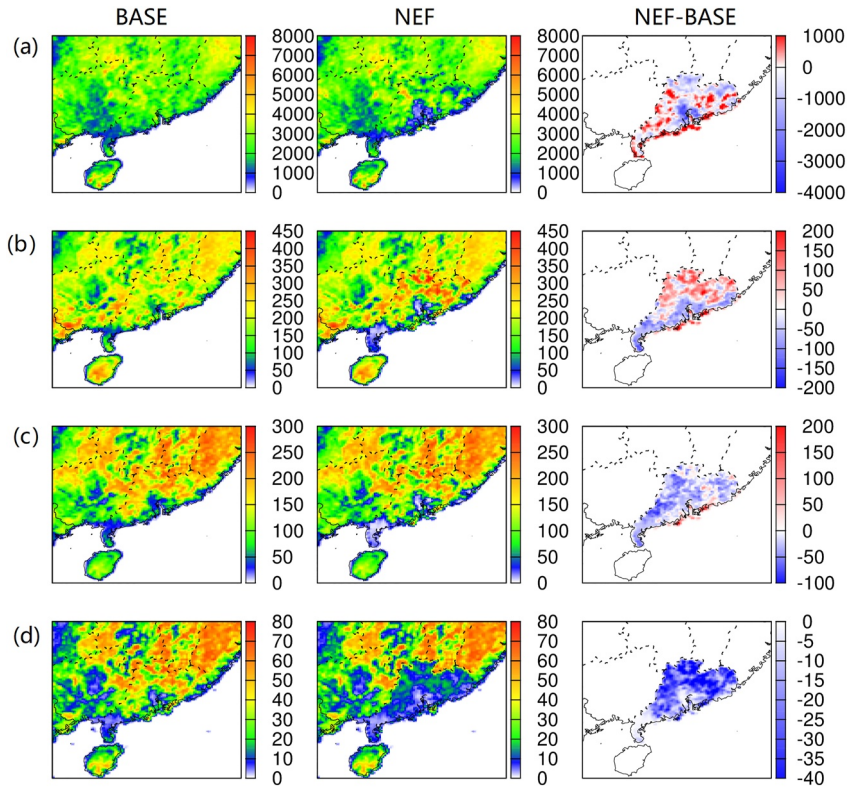

Figure 1. The EFs of BASE, NEF, and their difference (NEF-BASE) for (a) isoprene, (b) α-pinene, (c) β-pinene, and (d) β-caryophyllene. Units are ug m^{-2} h^{-1}.

emissions are 5-fold greater than those of monoterpenes, which is consistent with previous studies (Li et al., 2013; Wang et al., 2021a). In the PRD and its surrounding areas, the emission of isoprene is low, even in July, remaining below 0.5 mol s^{-1}. In winter, monoterpenes are also major contributors to the total BVOC emissions (the sum of isoprene, monoterpene, and sesquiterpene) with a contribution of over 30%.

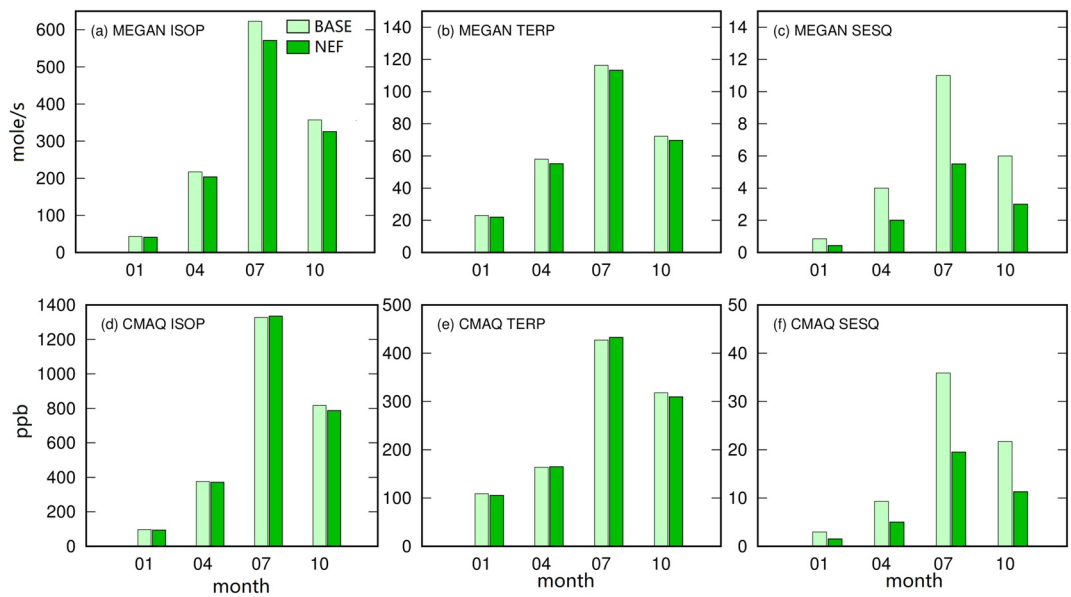

Figure 2. The comparison of total BVOC emissions and their concentrations of isoprene (ISOP), monoterpenes (TERP), and sesquiterpenes (SESQ) in GD from January to October 2019.

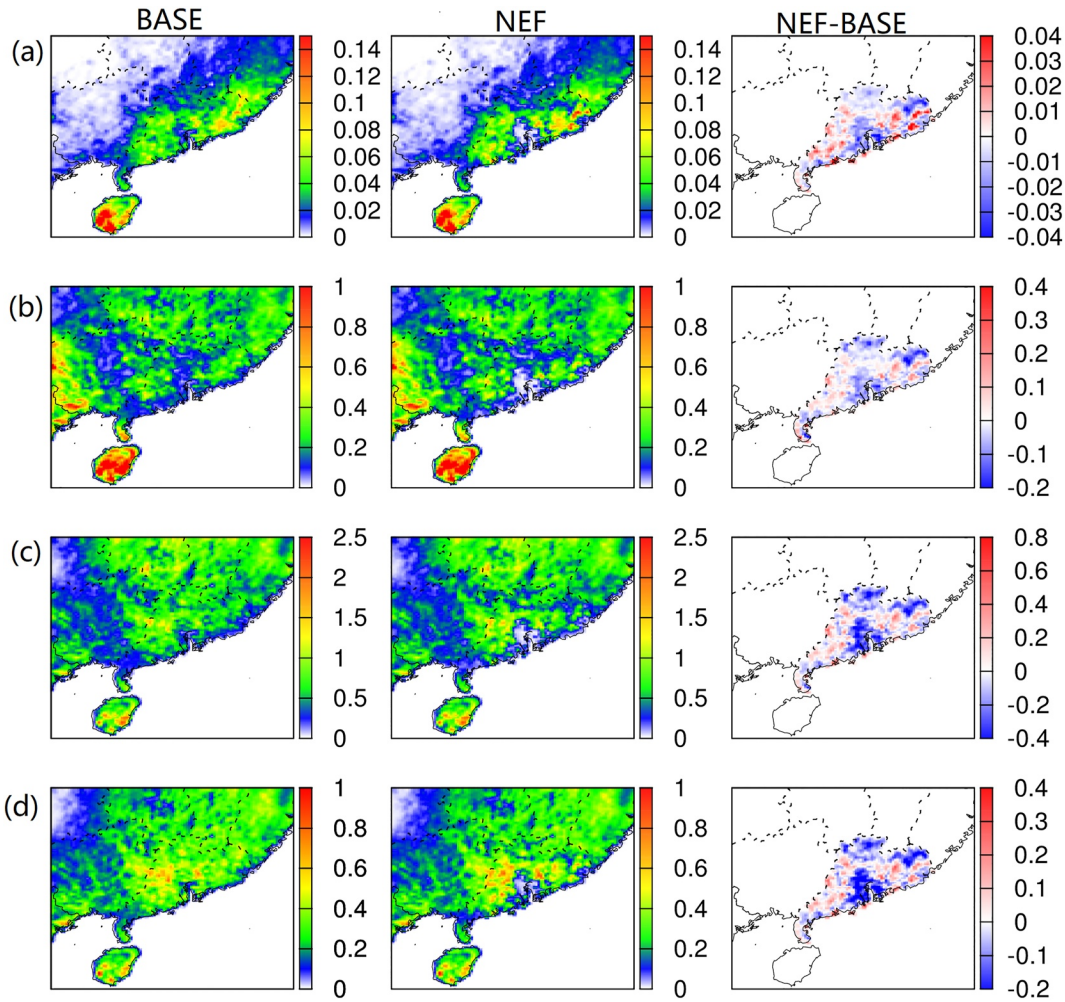

Figure 3. The isoprene emissions of BASE, NEF, and their difference (NEF-BASE) for (a) January, (b) April, (c) July, and (d) October. Units are mol s^{-1}.

On the regional scale, the NEF decreases major BVOCs emission rates in the PRD and its surrounding areas compared to that of the BASE case (Figures 2 and 3, Figures S6 and S7 in Supporting Information S1), which aligns with the findings of a previous study conducted in the same region (Situ et al., 2013). For isoprene, the reduction in NEF case is over 60%. In contrast, the higher isoprene emission rates are found in the west and east parts of the non-PRD region in GD, which is up to 0.6 mol s^{-1} larger than the BASE case in July. Besides the relatively high EFs, the high temperature (>30°C, Figure S8 in Supporting Information S1) also promotes isoprene emissions (Guenther et al., 2012), which further leads to higher concentrations (Figure S9 in Supporting Information S1). In west GD, the difference in isoprene concentration between the NEF and the BASE cases can reach ~+1 ppb. Unlike isoprene, monoterpene in the NEF case has higher emission rates in the north GD (Figure S6 in Supporting Information S1). In July, the NEF case estimates ~30% higher monoterpene emissions than the BASE case, and thus more monoterpene concentrations (up to +0.4 ppb) (Figure S10 in Supporting Information S1). Similar to EFs, substantially lower sesquiterpene emissions and concentrations are calculated in the NEF case through the study domain (Figure 2 and Figures S6 and S11 in Supporting Information S1).

3.3. O_3 and SOA Changes Due To BVOC EFs and Associated Impacts on AOC

In most areas of GD, the maximum daily 8 hr average (MDA8) O_3 is higher than 50 ppb in all simulation periods (Figure 4), exceeding Chinese national air quality standards Grade I (~47 ppb). Even in winter, when the BVOC emissions are low, the average MDA8 O_3 in south China can reach up to 45 ppb, which may be explained by the

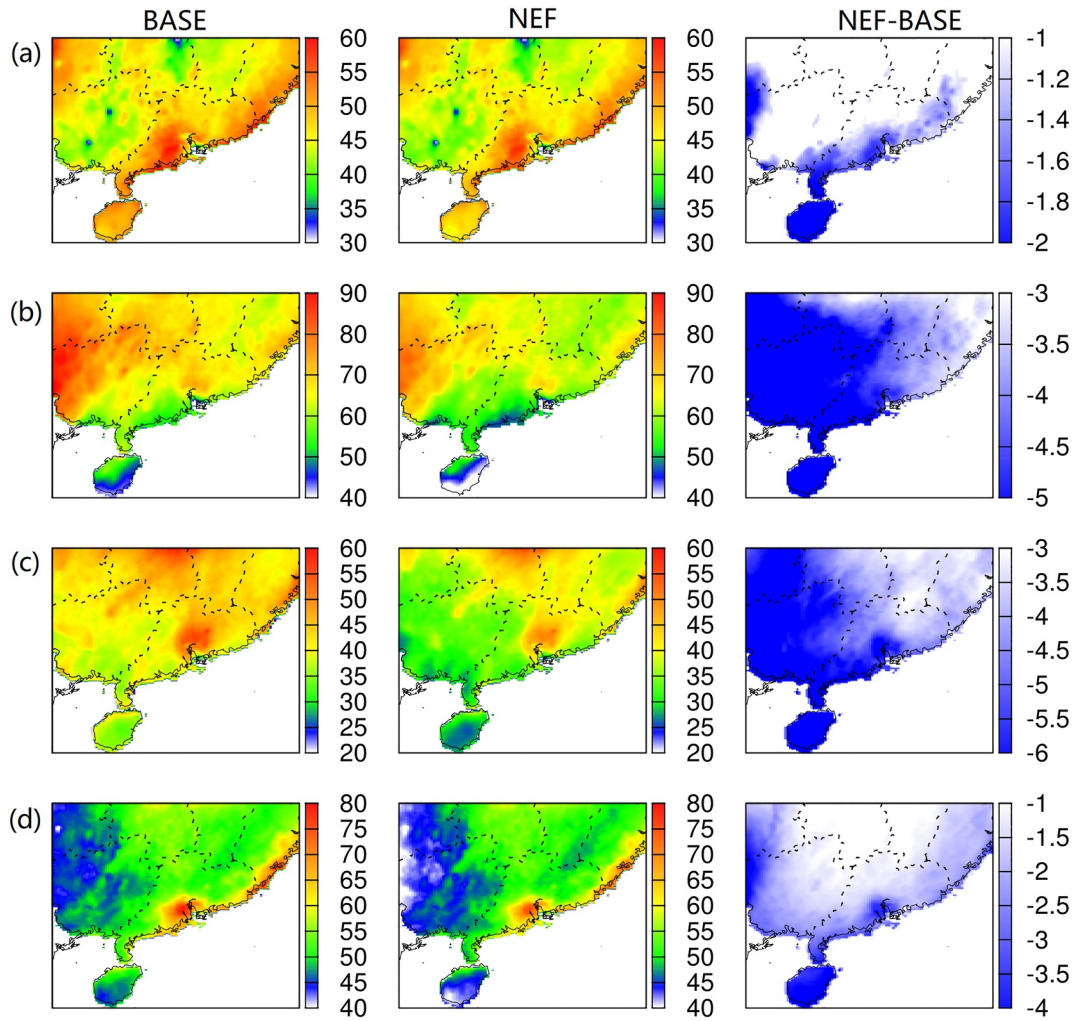

Figure 4. The CMAQ predicted MDA8 O_3 concentrations of BASE, NEF, and their difference (NEF-BASE) for (a) January, (b) April, (c) July, and (d) October. Units are ppb.

high temperature (>20°C) (Figure S8 in Supporting Information S1) in most of south China facilitates the O_3 formation. As an air pollution hotspot, the PRD region exhibits a consistent increase in O_3 concentrations, rising at a rate of 1.1 ppb a^{-1}. This surge notably surpasses the levels observed in major city clusters like the Sichuan Basin, which is largely attributed to the emerging BVOC emissions (Cao et al., 2022; Li et al., 2020a). The low levels of SOA occur in the summer in south China, but the concentration of biogenic SOA (BSOA) increases significantly at the same time (Figure 5 and Figure S12 in Supporting Information S1). In summer, the peak SOA concentration reaches 4 μg m^{-3} in the northern part of GD, which is approximately 4 times that in winter (Figure S12 in Supporting Information S1). Despite a significant reduction in total $PM_{2.5}$ levels in the PRD region, there has been a consistent rise in SOA concentrations over the past two decades, increasing at an average rate of 0.013 μg m^{-3} yr^{-1} (Cao et al., 2022; Shao et al., 2023). Moreover, distinct spatial distributions are simulated between these secondary pollutants (O_3 and SOA) and BVOC emissions. This difference is mainly attributed to the prevailing south wind during the high BVOC emission seasons, which enhances regional transport and brings more precursors to form the secondary pollutants in the northern part (Wang et al., 2018). To have in-depth understanding of the BVOC emissions on SOA, the changes in major BSOA components including BSOA from isoprene (IBSOA), monoterpenes (TBSOA), and sesquiterpenes (SBSOA) are also investigated (Figures S13–S15 in Supporting Information S1). In GD, the IBSOA plan an important role in the total BSOA, accounting for 63% and 65% of the annual BSOA in BASE and NEF cases, respectively. Notably, during winter, TBSOA contributes more to BSOA in both BASE and NEF cases compared to IBSOA. For all these BSOA components, the peak values are predicted in the autumn in northern GD, which is 3.3 times that of summer.

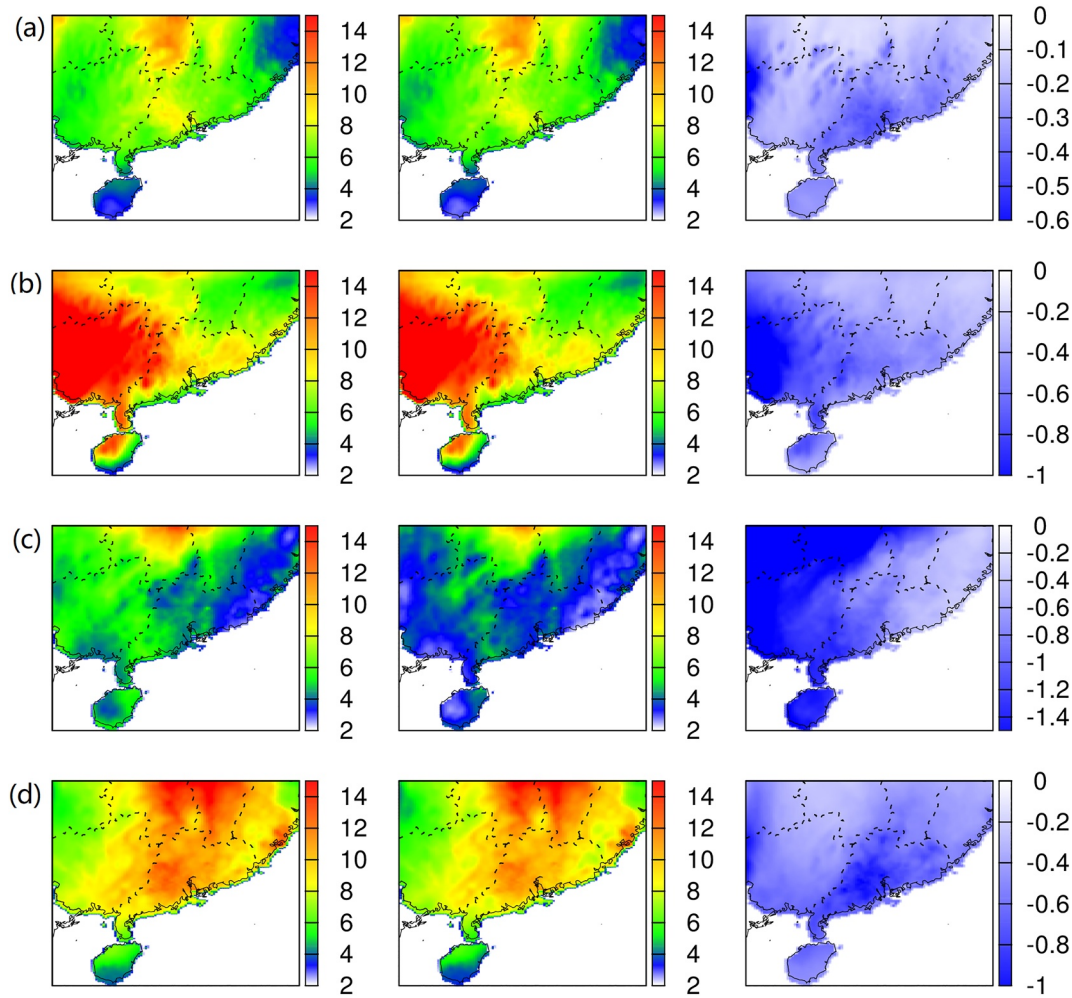

Figure 5. The CMAQ predicted SOA concentrations of BASE, NEF, and their difference (NEF-BASE) for (a) January, (b) April, (c) July, and (d) October. Units are μg m^{-3}.

From January to October, the lower MDA8 O_3 and SOA concentrations are predicted in the NEF case than in the BASE (Figures 4 and 5). The remarkable decreases are simulated in the west of south China in July, with a reduction of up to 6 ppb and 1.5 μg m^{-3} for MDA8 O_3 and SOA, respectively. Considering the O_3 sensitivity regime, no noticeable changes are found between the BASE and NEF cases (Figure S16 in Supporting Information S1). The PRD region is recognized as the VOC-limited region (Jin & Holloway, 2015), and thus the lower BVOC emissions reduce the O_3 concentration (∼−1 ppb) in this region (Figure S17 in Supporting Information S1). Compared to O_3, SOA concentrations are even more sensitive to the lower BVOC emissions in the NEF case (Figure S12 in Supporting Information S1). In particular, the declined BVOC emissions contribute more than 60% of the SOA reduction while causing less than 20% O_3 reduction on average. Considering the BSOA components, the NEF has the lower concentration than that of the BASE cases. Similar to SOA, the most remarkable decrease is found in SBSOA with the average reduction rate over 30%.

This study also investigates the changes in atmospheric oxidation capacity (AOC) by using different BVOC EFs (NEF and BASE cases). The AOC plays a significant role in the formation of secondary pollutants, which is able to give an in-depth understanding of the BVOC emissions on air quality. In the CMAQ model, the AOC refers to the sum of major oxidants such as OH, HO_2 and NO_3 radicals. In this study, the HO_x (sum of OH and HO_2) and NO_3 radical concentrations are used as the indicator to represent the AOC level. In most of south China, the lower HO_x concentrations in the NEF case during the daytime result in decreases in the secondary pollutants (Figure S18 in Supporting Information S1), which is consistent with previous studies (Ren et al., 2013; Zhu et al., 2021). Surprisingly, the NEF still predicts a higher HO_x concentration in a few

regions of GD, although the lower concentrations of secondary pollutants are found in entire south China. In these regions, the NEF case consistently predicts higher BVOC concentrations compared to the BASE case. This elevated BVOC presence leads to increased rates of oxidation reactions, subsequently heightening the HO_x levels. However, the resulting secondary pollutants, along with their precursors, might be transported to other locations due to regional dispersion, which could diminish the impact of the heightened HO_x. Previous study also indicated that the relationship between SOA and HO_x concentration is not unequivocally positive. Instances of low SOA concentration coinciding with high HO_x levels have been reported, highlighting the complexity of their interplay (Wang et al., 2021b). In addition, the HO_x diurnal variations are also investigated in the PRD major cities including Guangzhou, Shenzhen, and Zhuhai (Figure S19 in Supporting Information S1). Across these urban centers, HO_x exhibits comparable seasonal patterns, characterized by higher levels during summer and autumn and lower levels in winter. During summer and autumn, the peak concentration of HO_x typically transpires at midday, while in winter, it tends to occur during the night and afternoon. In Guangzhou, the rise in HO_x begins during spring, yet remains relatively stable compared to winter in the other cities. Notably, in all these locations, the diurnal concentration of HO_x is higher in the BASE case compared to the NEF. Specifically, the BASE predicts a 31% increase in HO_x concentration during summer noontime in Zhuhai compared to the NEF case. During the nighttime in the PRD region (Figure S20 in Supporting Information S1), lower NO_3 concentrations are predicted in the NEF case, primarily due to the lower O_3 levels (Figure S17 in Supporting Information S1), as NO_3 is mainly formed by the oxidation of NO_2 by O_3. A more comprehensive study is required to figure out the variations of AOC corresponding to BVOC emissions.

4. Conclusion

This study re-evaluates the BVOC emissions and their impacts on air quality in south China in 2019. An up-to-date localized BVOC EFs are measured for the MEGAN model in order to improve the accuracy of BVOC emission estimations (NEF case). The BVOC emission estimates as well as the model prediction of O_3 and SOA in south China were modeled with and without the updated EFs for comparison. The NEF case revealed reduced total BVOCs emissions, especially for sesquiterpenes with an average reduction rates up to 40%. More importantly, we found that with the updated BVOC emissions, O_3 prediction performance of the CMAQ model was improved with the MNB value dropping from 0.09 (BASE case) to 0.05 (NEF case) if comparing the O_3 levels from surface monitoring network with the modeled ones, signaling that the updating is in the right direction. In the NEF case with updated BVOC emissions, predicted concentrations of O_3 and SOA were reduced throughout south China, particularly in July in which predicted O_3 and SOA concentration could decrease by -6 ppb and -1.5 μg m^{-3}, respectively. This study suggests that EFs play a significant role in the BVOC emission estimates and thereby in air quality modeling, and localized EFs of BVOC could potentially improve model performance particularly in regions with higher forest coverage. It is worth noting that other factors, such as meteorology parameters, land-use types, leaf area index and atmospheric chemistry, might also contribute to uncertainties in BVOC emission estimates, more extensive investigations and evaluations are required in the future to combine field measurements, lab experiments, and modeling studies for in-depth understanding of the role of BVOC in atmosphere.

Conflict of Interest

The authors declare no conflicts of interest relevant to this study.

Data Availability Statement

The processed data of the ground-level observation data for the key pollutants in this paper are available at Zhu (2022). The reanalysis meteorological parameters data are available at (National Centers for Environmental Prediction/National Weather Service/NOAA/U.S. Department of Commerce, 2015). The Surface meteorological data for key parameters are available at Zhu (2023). The Multi-resolution Emission Inventory for China can be found at Zheng et al. (2021). The Localized BVOC EF and simulated data of O_3, SOA, and HOx data are publicly available at Wang (2023).

Acknowledgments
This work was supported by the National Natural Science Foundation of China (42022023/42321003), National Key Research and Development Program (2022YFC3703004/2022YFC3701103), the Hong Kong Research Grants Council (T24-504/17-N), Youth Innovation Promotion Association of the Chinese Academy of Sciences (Y2021096), Guangdong Foundation for Program of Science and Technology Research (2020B1111360001/2023B1212060049).

References

Bai, J., Guenther, A., Turnipseed, A., & Duhl, T. (2015). Seasonal and interannual variations in whole-ecosystem isoprene and monoterpene emissions from a temperate mixed forest in Northern China. *Atmospheric Pollution Research*, *6*(4), 696–707. https://doi.org/10.5094/APR.2015.078

Bai, J., Wang, M., John, G., & Ronald, G. P. (2001). A study of the nonmethane hydrocarbons at subtropical forest Part II: Diurnal variation. *Climatic and Environmental Research*, *6*(4), 456–466.

Baker, B., Bai, J. H., Johnson, C., Cai, Z. T., Li, Q. J., Wang, Y. F., et al. (2005). Wet and dry season ecosystem level fluxes of isoprene and monoterpenes from a southeast Asian secondary forest and rubber tree plantation. *Atmospheric Environment*, *39*(2), 381–390. https://doi.org/10.1016/j.atmosenv.2004.07.033

Bash, J. O., Baker, K. R., & Beaver, M. R. (2016). Evaluation of improved land use and canopy representation in BEIS v3.61 with biogenic VOC measurements in California. *Geoscientific Model Development*, *9*(6), 2191–2207. https://doi.org/10.5194/gmd-9-2191-2016

Cao, J., Situ, S., Hao, Y., Xie, S., & Li, L. (2022). Enhanced summertime ozone and SOA from biogenic volatile organic compound (BVOC) emissions due to vegetation biomass variability during 1981–2018 in China. *Atmospheric Chemistry and Physics*, *22*(4), 2351–2364. https://doi.org/10.5194/acp-22-2351-2022

Carlton, A. G., & Baker, K. R. (2011). Photochemical modeling of the Ozark isoprene volcano: MEGAN, BEIS, and their impacts on air quality predictions. *Environmental Science & Technology*, *45*(10), 4438–4445. https://doi.org/10.1021/es200050x

Carter, W. P. L., & Heo, G. (2013). Development of revised SAPRC aromatics mechanisms. *Atmospheric Environment*, *77*, 404–414. https://doi.org/10.1016/j.atmosenv.2013.05.021

Chen, C., Park, T., Wang, X., Piao, S., Xu, B., Chaturvedi, R. K., et al. (2019). China and India lead in greening of the world through land-use management. *Nature Sustainability*, *2*(2), 122–129. https://doi.org/10.1038/s41893-019-0220-7

Chen, Z., Chen, D., Zhao, C., Kwan, M. p., Cai, J., Zhuang, Y., et al. (2020). Influence of meteorological conditions on $PM_{2.5}$ concentrations across China: A review of methodology and mechanism. *Environment International*, *139*, 105558. https://doi.org/10.1016/j.envint.2020.105558

Emery, C., Tai, E., & Yarwood, G. (2001). Enhanced meteorological modeling and performance evaluation for two Texas ozone episodes. In *Prepared for the Texas natural resource conservation commission*. ENVIRON International Corporation.

Emmerson, K. M., Possell, M., Aspinwall, M. J., Pfautsch, S., & Tjoelker, M. G. (2020). Temperature response measurements from eucalypts give insight into the impact of Australian isoprene emissions on air quality in 2050. *Atmospheric Chemistry and Physics*, *20*(10), 6193–6206. https://doi.org/10.5194/acp-20-6193-2020

EPA, U. (2005). Guidance on the use of models and other analyses in attainment demonstrations for the 8-hour ozone NAAQS.

EPA, U. (2007). *Guidance on the use of models and other analyses for demonstrating attainment of air quality goals for ozone, $PM_{2.5}$, and regional haze*. US Environmental Protection Agency, Office of Air Quality Planning and Standards.

Fu, Y., & Liao, H. (2014). Impacts of land use and land cover changes on biogenic emissions of volatile organic compounds in China from the late 1980s to the mid-2000s: Implications for tropospheric ozone and secondary organic aerosol. *Tellus B: Chemical and Physical Meteorology*, *66*(1), 24987. https://doi.org/10.3402/tellusb.v66.24987

Fuentes, J. D., Gu, L., Lerdau, M., Atkinson, R., Baldocchi, D., Bottenheim, J. W., et al. (2000). Biogenic hydrocarbons in the atmospheric boundary layer: A review. *Bulletin of the American Meteorological Society*, *81*(7), 1537–1576. https://doi.org/10.1175/1520-0477(2000)081<1537:Bhitab>2.3.Co;2

Geron, C., Harley, P., & Guenther, A. (2001). Isoprene emission capacity for US tree species. *Atmospheric Environment*, *35*(19), 3341–3352. https://doi.org/10.1016/S1352-2310(00)00407-6

Guenther, A., Hewitt, C. N., Erickson, D., Fall, R., Geron, C., Graedel, T., et al. (1995). A global model of natural volatile organic compound emissions. *Journal of Geophysical Research*, *100*(D5), 8873–8892. https://doi.org/10.1029/94JD02950

Guenther, A., Jiang, X., Shah, T., Huang, L., Kemball-Cook, S., & Yarwood, G. (2020). Model of emissions of gases and aerosol from nature version 3 (MEGAN3) for estimating biogenic emissions. In *Paper presented at air pollution modeling and its application XXVI*. Springer International Publishing.

Guenther, A. B., Jiang, X., Heald, C. L., Sakulyanontvittaya, T., Duhl, T., Emmons, L. K., & Wang, X. (2012). The model of emissions of gases and aerosols from nature version 2.1 (MEGAN2.1): An extended and updated framework for modeling biogenic emissions. *Geoscientific Model Development*, *5*(6), 1471–1492. https://doi.org/10.5194/gmd-5-1471-2012

Guenther, A. B., Zimmerman, P. R., Harley, P. C., Monson, R. K., & Fall, R. (1993). Isoprene and monoterpene emission rate variability: Model evaluations and sensitivity analyses. *Journal of Geophysical Research*, *98*(D7), 12609–12617. https://doi.org/10.1029/93JD00527

Hantson, S., Knorr, W., Schurgers, G., Pugh, T. A. M., & Arneth, A. (2017). Global isoprene and monoterpene emissions under changing climate, vegetation, CO_2 and land use. *Atmospheric Environment*, *155*, 35–45. https://doi.org/10.1016/j.atmosenv.2017.02.010

Hu, J., Chen, J., Ying, Q., & Zhang, H. (2016). One-year simulation of ozone and particulate matter in China using WRF/CMAQ modeling system. *Atmospheric Chemistry and Physics*, *16*(16), 10333–10350. https://doi.org/10.5194/acp-16-10333-2016

Huang, L., McGaughey, G., McDonald-Buller, E., Kimura, Y., & Allen, D. T. (2015). Quantifying regional, seasonal and interannual contributions of environmental factors on isoprene and monoterpene emissions estimates over eastern Texas. *Atmospheric Environment*, *106*, 120–128. https://doi.org/10.1016/j.atmosenv.2015.01.072

Huang, Y., Ho, S. S. H., Ho, K. F., Lee, S. C., Gao, Y., Cheng, Y., & Chan, C. S. (2011). Characterization of biogenic volatile organic compounds (BVOCs) in cleaning reagents and air fresheners in Hong Kong. *Atmospheric Environment*, *45*(34), 6191–6196. https://doi.org/10.1016/j.atmosenv.2011.08.012

Jiang, X., Guenther, A., Potosnak, M., Geron, C., Seco, R., Karl, T., et al. (2018). Isoprene emission response to drought and the impact on global atmospheric chemistry. *Atmospheric Environment*, *183*, 69–83. https://doi.org/10.1016/j.atmosenv.2018.01.026

Jin, X., & Holloway, T. (2015). Spatial and temporal variability of ozone sensitivity over China observed from the ozone monitoring instrument. *Journal of Geophysical Research: Atmospheres*, *120*(14), 7229–7246. https://doi.org/10.1002/2015JD023250

Leung, D. Y. C., Wong, P., Cheung, B. K. H., & Guenther, A. (2010). Improved land cover and emission factors for modeling biogenic volatile organic compounds emissions from Hong Kong. *Atmospheric Environment*, *44*(11), 1456–1468. https://doi.org/10.1016/j.atmosenv.2010.01.012

Li, K., Jacob, D. J., Shen, L., Lu, X., De Smedt, I., & Liao, H. (2020a). Increases in surface ozone pollution in China from 2013 to 2019: Anthropogenic and meteorological influences. *Atmospheric Chemistry and Physics*, *20*(19), 11423–11433. https://doi.org/10.5194/acp-20-11423-2020

Li, L., Yang, W., Xie, S., & Wu, Y. (2020b). Estimations and uncertainty of biogenic volatile organic compound emission inventory in China for 2008–2018. *Science of the Total Environment*, *733*, 139301. https://doi.org/10.1016/j.scitotenv.2020.139301

Li, L. Y., Chen, Y., & Xie, S. D. (2013). Spatio-temporal variation of biogenic volatile organic compounds emissions in China. *Environmental Pollution*, *182*, 157–168. https://doi.org/10.1016/j.envpol.2013.06.042

Liu, M., Wang, Z., Li, S., Lü, X., Wang, X., & Han, X. (2017). Changes in specific leaf area of dominant plants in temperate grasslands along a 2500-km transect in northern China. *Scientific Reports*, *7*(1), 10780. https://doi.org/10.1038/s41598-017-11133-z

Liu, Y., & Wang, T. (2020). Worsening urban ozone pollution in China from 2013 to 2017 – Part 1: The complex and varying roles of meteorology. *Atmospheric Chemistry and Physics*, *20*(11), 6305–6321. https://doi.org/10.5194/acp-20-6305-2020

Lun, X., Lin, Y., Chai, F., Fan, C., Li, H., & Liu, J. (2020). Reviews of emission of biogenic volatile organic compounds (BVOCs) in Asia. *Journal of Environmental Sciences*, *95*, 266–277. https://doi.org/10.1016/j.jes.2020.04.043

Ma, M., Gao, Y., Wang, Y., Zhang, S., Leung, L. R., Liu, C., et al. (2019). Substantial ozone enhancement over the North China Plain from increased biogenic emissions due to heat waves and land cover in summer 2017. *Atmospheric Chemistry and Physics*, *19*(19), 12195–12207. https://doi.org/10.5194/acp-19-12195-2019

Misztal, P. K., Avise, J. C., Karl, T., Scott, K., Jonsson, H. H., Guenther, A. B., & Goldstein, A. H. (2016). Evaluation of regional isoprene emission factors and modeled fluxes in California. *Atmospheric Chemistry and Physics*, *16*(15), 9611–9628. https://doi.org/10.5194/acp-16-9611-2016

National Centers for Environmental Prediction/National Weather Service/NOAA/U.S. Department of Commerce. (2015). NCEP GDAS/FNL 0.25 degree global tropospheric analyses and forecast grids (updated daily) [Dataset]. Research Data Archive at the National Center for Atmospheric Research, Computational and Information Systems Laboratory. https://doi.org/10.5065/D65Q4T4Z

Oderbolz, D. C., Aksoyoglu, S., Keller, J., Barmpadimos, I., Steinbrecher, R., Skjøth, C. A., et al. (2013). A comprehensive emission inventory of biogenic volatile organic compounds in Europe: Improved seasonality and land-cover. *Atmospheric Chemistry and Physics*, *13*(4), 1689–1712. https://doi.org/10.5194/acp-13-1689-2013

Opacka, B., Müller, J. F., Stavrakou, T., Bauwens, M., Sindelarova, K., Markova, J., & Guenther, A. B. (2021). Global and regional impacts of land cover changes on isoprene emissions derived from spaceborne data and the MEGAN model. *Atmospheric Chemistry and Physics*, *21*(11), 8413–8436. https://doi.org/10.5194/acp-21-8413-2021

Pressley, S., Lamb, B., Westberg, H., & Vogel, C. (2006). Relationships among canopy scale energy fluxes and isoprene flux derived from long-term, seasonal eddy covariance measurements over a hardwood forest. *Agricultural and Forest Meteorology*, *136*(3), 188–202. https://doi.org/10.1016/j.agrformet.2004.11.013

Purser, G., Drewer, J., Heal, M. R., Sircus, R. A. S., Dunn, L. K., & Morison, J. I. L. (2021). Isoprene and monoterpene emissions from alder, aspen and spruce short-rotation forest plantations in the United Kingdom. *Biogeosciences*, *18*(8), 2487–2510. https://doi.org/10.5194/bg-18-2487-2021

Ren, X., van Duin, D., Cazorla, M., Chen, S., Mao, J., Zhang, L., et al. (2013). Atmospheric oxidation chemistry and ozone production: Results from SHARP 2009 in Houston, Texas. *Journal of Geophysical Research: Atmospheres*, *118*(11), 5770–5780. https://doi.org/10.1002/jgrd.50342

Shao, T., Wang, P., Yu, W., Gao, Y., Zhu, S., Zhang, Y., et al. (2023). Drivers of alleviated $PM_{2.5}$ and O_3 concentrations in China from 2013 to 2020. *Resources, Conservation and Recycling*, *197*, 107110. https://doi.org/10.1016/j.resconrec.2023.107110

Sharkey, T. D., Singsaas, E. L., Lerdau, M. T., & Geron, C. D. (1999). Weather effects on isoprene emission capacity and applications in emission algorithms. *Ecological Applications*, *9*(4), 1132–1137. https://doi.org/10.1890/1051-0761(1999)009[1132:WEOIEC]2.0.CO;2

Situ, S., Guenther, A., Wang, X., Jiang, X., Turnipseed, A., Wu, Z., et al. (2013). Impacts of seasonal and regional variability in biogenic VOC emissions on surface ozone in the Pearl River delta region, China. *Atmospheric Chemistry and Physics*, *13*(23), 11803–11817. https://doi.org/10.5194/acp-13-11803-2013

Tsui, J. K.-Y., Guenther, A., Yip, W.-K., & Chen, F. (2009). A biogenic volatile organic compound emission inventory for Hong Kong. *Atmospheric Environment*, *43*(40), 6442–6448. https://doi.org/10.1016/j.atmosenv.2008.01.027

Tuazon, E. C., & Atkinson, R. (1990). A product study of the gas-phase reaction of Isoprene with the OH radical in the presence of NOx. *International Journal of Chemical Kinetics*, *22*(12), 1221–1236. https://doi.org/10.1002/kin.550221202

Vukovich, J., & Pierce, T. (2002). The implementation of BEIS3 within the SMOKE modeling framework.

Wang, H., Wu, Q., Guenther, A. B., Yang, X., Wang, L., Xiao, T., et al. (2021a). A long-term estimation of biogenic volatile organic compound (BVOC) emission in China from 2001–2016: The roles of land cover change and climate variability. *Atmospheric Chemistry and Physics*, *21*(6), 4825–4848. https://doi.org/10.5194/acp-21-4825-2021

Wang, P. (2023). Localized BVOC EF and simulated data of O_3, SOA, and HOx data [Dataset]. figshare. https://doi.org/10.6084/m9.figshare.24077757.v1

Wang, P., Chen, Y., Hu, J., Zhang, H., & Ying, Q. (2019). Attribution of tropospheric ozone to NOx and VOC emissions: Considering ozone formation in the transition regime. *Environmental Science & Technology*, *53*(3), 1404–1412. https://doi.org/10.1021/acs.est.8b05981

Wang, P., Liu, Y., Dai, J., Fu, X., Wang, X., Guenther, A., & Wang, T. (2021b). Isoprene emissions response to drought and the impacts on ozone and SOA in China. *Journal of Geophysical Research: Atmospheres*, *126*(10), e2020JD033263. https://doi.org/10.1029/2020JD033263

Wang, P., Schade, G., Estes, M., & Ying, Q. (2017). Improved MEGAN predictions of biogenic isoprene in the contiguous United States. *Atmospheric Environment*, *148*, 337–351. https://doi.org/10.1016/j.atmosenv.2016.11.006

Wang, P., Ying, Q., Zhang, H., Hu, J., Lin, Y., & Mao, H. (2018). Source apportionment of secondary organic aerosol in China using a regional source-oriented chemical transport model and two emission inventories. *Environmental Pollution*, *237*, 756–766. https://doi.org/10.1016/j.envpol.2017.10.122

Wang, S., Zhang, Y., Ma, J., Zhu, S., Shen, J., Wang, P., & Zhang, H. (2021c). Responses of decline in air pollution and recovery associated with COVID-19 lockdown in the Pearl River Delta. *Science of the Total Environment*, *756*, 143868. https://doi.org/10.1016/j.scitotenv.2020.143868

Wang, X., Situ, S., Chen, W., Zheng, J., Guenther, A., Fan, Q., & Chang, M. (2016). Numerical model to quantify biogenic volatile organic compound emissions: The Pearl River Delta region as a case study. *Journal of Environmental Sciences*, *46*, 72–82. https://doi.org/10.1016/j.jes.2015.08.032

Wang, X., Situ, S., Guenther, A., Chen, F., Wu, Z., Xia, B., & Wang, T. (2011). Spatiotemporal variability of biogenic terpenoid emissions in Pearl River Delta, China, with high-resolution land-cover and meteorological data. *Tellus B: Chemical and Physical Meteorology*, *63*(2), 241–254. https://doi.org/10.1111/j.1600-0889.2011.00523.x

Yang, J., & Zhao, Y. (2023). Performance and application of air quality models on ozone simulation in China – A review. *Atmospheric Environment*, *293*, 119446. https://doi.org/10.1016/j.atmosenv.2022.119446

Ying, Q., Li, J., & Kota, S. H. (2015). Significant contributions of isoprene to summertime secondary organic aerosol in eastern United States. *Environmental Science & Technology*, *49*(13), 7834–7842. https://doi.org/10.1021/acs.est.5b02514

Zeng, J., Song, W., Zhang, Y., Mu, Z., Pang, W., Zhang, H., & Wang, X. (2022a). Emissions of isoprenoids from dominant tree species in subtropical China. *Frontiers in Forests and Global Change*, *5*. https://doi.org/10.3389/ffgc.2022.1089676

Zeng, J., Zhang, Y., Zhang, H., Song, W., Wu, Z., & Wang, X. (2022b). Design and characterization of a semi-open dynamic chamber for measuring biogenic volatile organic compound (BVOC) emissions from plants. *Atmospheric Measurement Techniques*, *15*(1), 79–93. https://doi.org/10.5194/amt-15-79-2022

Zhang, R., White, A. T., Pour Biazar, A., McNider, R. T., & Cohan, D. S. (2018). Incorporating GOES satellite photosynthetically active radiation (PAR) retrievals to improve biogenic emission estimates in Texas. *Journal of Geophysical Research: Atmospheres*, *123*(2), 1309–1324. https://doi.org/10.1002/2017JD026792

Zhang, Y., Huang, J.-P., Henze, D. K., & Seinfeld, J. H. (2007). Role of isoprene in secondary organic aerosol formation on a regional scale. *Journal of Geophysical Research*, *112*(D20), D20207. https://doi.org/10.1029/2007JD008675

Zhang, Y., Zhang, R., Yu, J., Zhang, Z., Yang, W., Zhang, H., et al. (2020). Isoprene mixing ratios measured at twenty sites in China during 2012–2014: Comparison with model simulation. *Journal of Geophysical Research: Atmospheres*, *125*(24), e2020JD033523. https://doi.org/10.1029/2020JD033523

Zheng, B., Zhang, Q., Geng, G., Chen, C., Shi, Q., Cui, M., et al. (2021). Changes in China's anthropogenic emissions and air quality during the COVID-19 pandemic in 2020 [Dataset]. Earth System Science Data, *13*(6), 2895–2907. https://doi.org/10.5194/essd-13-2895-2021

Zheng, J., Zheng, Z., Yu, Y., & Zhong, L. (2010). Temporal, spatial characteristics and uncertainty of biogenic VOC emissions in the Pearl River Delta region, China. *Atmospheric Environment*, *44*(16), 1960–1969. https://doi.org/10.1016/j.atmosenv.2010.03.001

Zhu, S. (2022). Observational data [Dataset]. figshare. https://doi.org/10.6084/m9.figshare.21709265.v1

Zhu, S. (2023). Surface meteorological data for key parameters [Dataset]. figshare. https://doi.org/10.6084/m9.figshare.22439086.v1

Zhu, S., Poetzscher, J., Shen, J., Wang, S., Wang, P., & Zhang, H. (2021). Comprehensive insights into O_3 changes during the COVID-19 from O_3 formation regime and atmospheric oxidation capacity. *Geophysical Research Letters*, *48*(10), e2021GL093668. https://doi.org/10.1029/2021GL093668

Erratum

The originally published version of this article contained errors in the affiliations. Coauthors Peng Wang and Haixing Gong are affiliated with the Department of Atmospheric and Oceanic Sciences, Fudan University, Shanghai, China. Coauthors Yanli Zhang, Jianqiang Zeng, and Xinming Wang are affiliated with the State Key Laboratory of Organic Geochemistry and Guangdong Key Laboratory of Environmental Protection and Resources Utilization, Guangzhou Institute of Geochemistry, Chinese Academy of Sciences, Guangzhou, China. Coauthor Hongliang Zhang is affiliated with the Institute of Eco-Chongming (IEC), Shanghai, China; the IRDR ICoE on Risk Interconnectivity and Governance on Weather/Climate Extremes Impact and Public Health, Fudan University, Shanghai, China; and the Shanghai Key Laboratory of Atmospheric Particle Pollution and Prevention, Department of Environmental Science and Engineering, Fudan University, Shanghai, China. Coauthor Alex Guenther is affiliated with the Department of Earth System Science, University of California, Irvine, Irvine, CA, USA. Coauthor Tao Wang is affiliated with the Department of Civil and Environmental Engineering, Hong Kong Polytechnic University, Hong Kong, China. The affiliations have been corrected, and this may be considered the authoritative version of record.